

Measurement of field-emission properties of a single crystallized silicon emitter using scanning electronic microscopy

T.C. Cheng^{a)}, H.T. Hsueh, W.J Huang, and M. N. Chang

National Nano Devices Laboratories, 1001-1 Ta-Hsueh Road, Hsinchu, Taiwan, 30050, R.O.C.

J. S. Wu

National Chaio Tung University, Hsinchu, Taiwan 30010, R.O.C.

S.C. Kung

Industrial Technology Research Institute³, Chung Hsing Rd., Chutung, Hsinchu, Taiwan, R.O.C.

Abstract

Comparison of field emission properties between single silicon emitter and silicon emitters array are investigated in this letter by utilizing a scanning electron microscopy (SEM) with a small tungstenic probe having apex radius approximately 90nm. Interelectrode distance is controlled within tens of nanometers. Measured I-V data fitted using Fowler-Nordheim model revealed that the turn-on field of an individual emitter is much higher than that of emitter array consisting of 288 nearly identical emitters. This observation is further supported by the simplified electric-field calculation. Experimental results also indicate that the anode area may be an important factor of in determining field emission.

a) Electronic email: tccheng@mail.ndl.org.tw

Field-emission properties have been studied intensively for various materials in the past decade, in which performance was found to strongly depend on the inherence, morphology [1] and the density of materials [2], to name a few. Materials used for electron emission, such as diamond, diamond like carbon (DLC), and carbon nanotubes (CNTs) on silicon wafer, have been demonstrated for possible commercial applications [3-5]. Therefore, electron emission based on silicon materials is also of great importance due to the advantage in integrating silicon-based vacuum microelectronics and silicon integrated circuit technology.

Several commercial applications have been proposed using the field emission phenomena such as field emission display, microwave power devices, and electron gun in various visualization equipments [6-8]. Past studies found that emission characteristics of field emitters depend on tip sharpness, emitter material, aspect ratio of tip and their surface conditions [9-12]. Many field-emission measurement techniques are developed for dealing with different applications. For example, Gangloff et al. [13] used the metal-ball anode (250 μ m in diameter) to measure the self-aligned, gate arrays of individual nanotube and nanowire emitters. Bonard [14] measured the field emission of an individual carbon nanotube using SEM, and found that both the geometry of the carbon nanotube and electrode distance between carbon nanotube and anode are the important factors for field emission. In addition, results

from these studies also showed that the density of emitters determines the performance of emission devices. However, the measured field-emission properties often result from a specific area of CNTs or a bundle of carbon nanofibers (CNFs), mainly because the uniformity of carbon nanotubes is difficult to control in practice and the anode area is much larger than the actual emitting areas of CNT tubes. For understanding the mechanism between the emitters and anode, it is interesting to measure the field-emission properties between total emission area and a single emitter. In this letter, the silicon nanotip array that is much easier to control its uniformity and geometry is used as the emitters for the measurement of field-emission properties using scanning electron microscopy.

The emitter array is fabricated by ICP dry plasma etching with three-step procedures. First, after RCA clean, a 10 μ m circular AZ4620 photoresist mask is patterned by anisotropic etching to produce high aspect ratio circular rods (25 μ m height). Etching was carried out in a commercial vertical reactor (Oxford plasma Lab 100) using a mixture of SF₆ and O₂ with higher RF power because of higher ion bombardment. Second, isotropic etching, as shown in Fig. 1(a), is used to produce sharp emitters by undercutting effect under the mask with proper plasma control. In this procedure, higher SF₆ concentration is necessary to make the isotropic etching by the chemical reaction between SF₆ and silicon rods. Finally, the silicon tips are placed

in the furnace for oxidation and then are removed by BOE wet etching to make the nanotip array. In addition, wet etching by BOE also ensures that there is no negative oxide layer on the surface of nanotip. Negative oxide layer shall degrade the field-emission performance and the reliability of the emitter [15], thus, making the Fowler-Nordheim plot nonlinear [16]. Each emitter, as shown in Fig. 1(b), purposely arranged in a periodic manner, has the same field enhancement factor, β , depending on the emitter geometry, which has the same contribution for emission current according to the Edgcombe relation[17],

$$\beta = 1.2 \left(2.5 + \frac{h}{r} \right)^{0.9} \quad (1)$$

where h and r represent the height of the emitter, and radius at the apex, respectively.

To measure the field-emission properties of a single emitter, a tungsten probe is fabricated by electrolysis with KOH solution. First we cut the tungsten filament about 1cm in length and clip it on the anode of the electrobath. Second, we turn on the power supply with certain power such that the electrolysis occurs in the KOH electrobath. During this process, light emission occurs due to the reaction of the tungsten filament with the KOH solution. Nanotungsten probe can be formed once the light emission disappears. As shown in Fig. 1(b), the diameter and apex radius of tungsten anode was 1 μ m and 90nm, respectively. Besides, the concentration of KOH

solution is a key factor in forming a sharp tip.

The single emitter was measured by a vacuum field emission apparatus, which could be controlled with distance between the emitter and anode within the accuracy of nanometer order in the in-situ image of SEM. The nanotungsten probe installed on the nanomotor is used as the anode of silicon tip. For aligning the emitter with the anode apex, we could first focus on the emitter apex and then drive the piezoelectric nanomotor to move the anode into the required position. Alignment is not considered to be correct until the apex of anode is clearly shown by real imaging of SEM. In this single emitter measurement, the electrode distance between these two apices is maintained at 46nm throughout the study, unless otherwise specified. Applied voltage on the anode, with substrate grounded, ranges from 0 to 250 volts, while the chamber pressure is kept lower than 9.6×10^{-7} torr. In contrast, corresponding experiment with large flat anode is done without SEM control. For this experiment, distance between anode and the sample is maintained at 50 μ m with maximum applied voltage at 1000 volts.

Typical results of electron field-emission properties of the single tungsten nanotip to single silicon emitter and flat plate to silicon emitter array (288 emitters) are illustrated, respectively, in Fig. 2(a) and Fig. 2(b). Figure 2(a) shows the I-V characteristics of a single silicon emitter with the corresponding Fowler-Nordheim

plot (FN plot) as the inset. Maximum voltage applied at the anode is constrained to be less than 250 volts because the high anode resistance results in the meltdown of the tungsten nanotip when higher voltage is applied. Emission current density is calculated using the cross section of the tungsten anode as emission area achieves J_e as $10\text{nA}/\mu\text{m}^2$, under $3913.04\text{V}/\mu\text{m}$ applied field which is close to the result analyzed using Fowler-Nordheim model (FN model) as $4039.1\text{ V}/\mu\text{m}$ [18]. Furthermore, in the current case, the FN plot can be written as

$$FN \text{ plot} = \frac{-6.44 \times 10^9 \phi^{1.5}}{\beta} \quad (2)$$

where ϕ is 4.52eV as the work function of silicon emitter and β is the field enhancement factor. As shown in equation (2), using typical value encountered in silicon emitter, one obtains the field enhancement factor of 1.3. In addition, the emission properties of corresponding experiment using a large flat anode are shown in Fig. 2(b) with the associated FN plot as the inset. Turn-on field for emission of the silicon emitters is about $16\text{ V}/\mu\text{m}$ from the direct calculation and is very close to the $15\text{ V}/\mu\text{m}$ from the FN model. Resulting fitted value of field enhancement factor from the FN plot is $\beta = 386$. By comparing these two experiments, the turn-on field of a single emitter using tungsten nanotip is extraordinarily higher than that of the emitter array using large plate anode.

To further understand the experimental findings, simplified two-dimensional

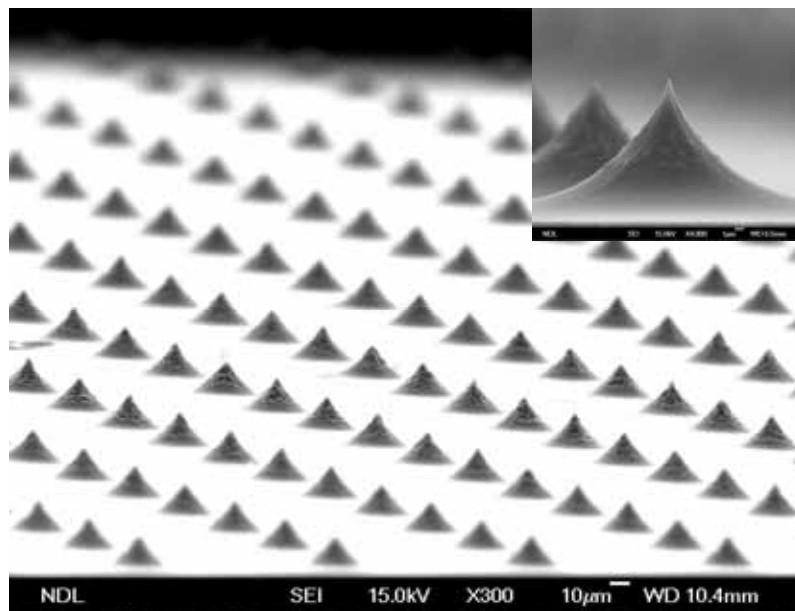
electrostatic field are simulated, respectively, for the two configurations we are interested in. Resulting distributions of electrostatic field are shown in Fig. 4. In Fig. 4(a), calculations show that the extraordinarily high field between the emitter and the tungsten anode is about 4057-4565V/ μm . Distribution of turn-on electric field (4039.1V/ μm) is restricted and confined at a very small distance between the apexes of the emitter and anode. It is implied that the electrons emit from the silicon nanotip to the tungsten anode is confined in a small region, which depends on the size of the vacuum gap between tip and anode. On the other hand, as shown in Fig. 4(b), there exists different distribution of electric field for the case of the silicon tip using large flat anode. As expected, highest electric field occurs at the top of the each silicon emitter with a value of 58V/ μm . It is clearly shown that most of the average field between emitters and flat anode is in the range of 14~16V/ μm . According to the experimental result as shown in Fig. 2(b), the electrons can emit from the silicon emitters if the local electrostatic field is greater than the turn-on field (15 V/ μm). The simulation results indicate that the emission current measured from the flat anode results from the contribution of all silicon emitters. It is interesting to note that the emission phenomenon not only depends on the density and geometry of emitter [2], but also depends on the geometry of anode because it can change the distribution of electrostatic field.

In summary, the turn-on field emission behavior of a single emitter is revealed by utilizing scanning electron microscopy with a tungsten nanotip anode. Comparing with the experimental and calculated results, the turn-on field analyzed by Fowler-Nordheim model is similar to the calculated results with large flat anode and nano-tungsten anode. By following the FN law, the extracted field enhancement factor for a single silicon emitter measurement is low when compared with that obtained using large plate anode. In addition, it is important to point out that the field emission performance is also affected by geometry of the anode.

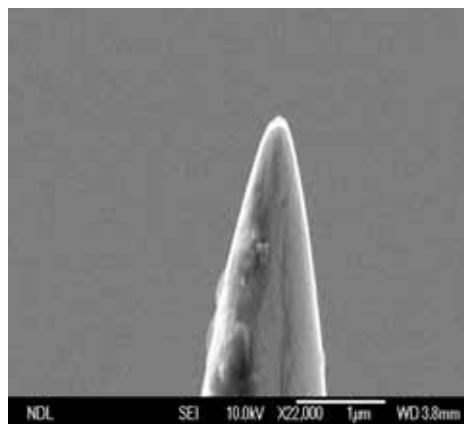
The authors wish to thank Dr. Volker Klocke, and Dr. Andreas Rosenberger, now at the Klocke Nanotechnik, for their technical support. We are also grateful to Mr. Frank Mak at Tricopek for their encouragement and discussion.

References

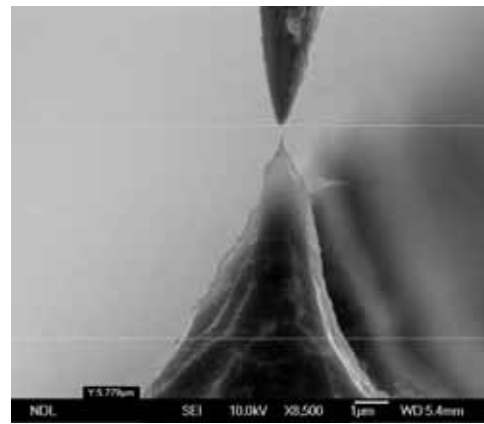
- [1] K.L. Ng, J. Yuan, J.T. Cheung, K.W. Cheah, Solid State Commun. 123 (2002) 205.
- [2] L. Nillson, O. Groening, C. Emmenegger, O. Kuettel, E. Schaller, L. Schlapbach, Appl. Phys. Lett. 76 (2000) 2071.
- [7] M.R. Rakhshandehroo, J.W. Weigold, W.C. Tian, S.W. Pang, J. Vac. Sci. Technol. B 16 (1998) 2849.
- [8] M.R. Rakhshandehroo, S.W. Pang, IEEE Trans. Electron Devices 46 (1999) 797.
- [9] D. Temple, Mater. Sci. Engng, Reports: Rev. J. 24 (1999) 185.
- [3] I. Brodie, C.A. Spindt, Adv. Electron. Electron Phys. 83 (1992) 1.
- [4] C.E. Holland, et al., IEEE Trans. Electron Devices 38 (1991) 2368.
- [5] P.R. Schwoebel, I. Brodie, J. Vac. Sci. Technol. B 13 (1995) 1391.
- [6] C.A. Spindt, et al., J. Appl. Phys. 47 (1976) 5248.
- [10] Vladimir I. Merkulov, Douglas H. Lowndes, Larry R. Baylor, J. Appl. Phys 89 (2001) 1933
- [11] M. A. Guillorn, A.V. Melechko, V.I. Merkulov, D.K. Hensley, M.L. Simpson, D.H. Lowndes, Appl. Phys. Lett. 81 (2002) 3660.
- [12] M. A. Guillorn, A.V. Melechko, V.I. Merkulov, E.D. Ellis, C.L. Britton, M.L. Simpson, D.H. Lowndes, L.R. Baylor, Appl. Phys. Lett. 79 (2001) 3506
- [13] L. Gangloff, E. Minoux, -----, Nano Lett. ,
- [14] J. M. Bonard, K. A. Dean, B. F. Coll and C. Klinke, Phys. Rev. Lett. , 89, 197602 (2002).
- [15] L. Chen, M. M. El-Gomati, Ultramicroscopy, 79 (1999) 135.
- [16] Q. A. Huang, Applied surface science, 93 (1996) 77.
- [17] C. J. Edgcombe and U. Valdré, Philos. Mag. B 82 (2002) 987.
- [18] J. W. Gaszuk and E. W. Plummer, Rev. Mod. Phys. 45, 487 (1973)



(a)

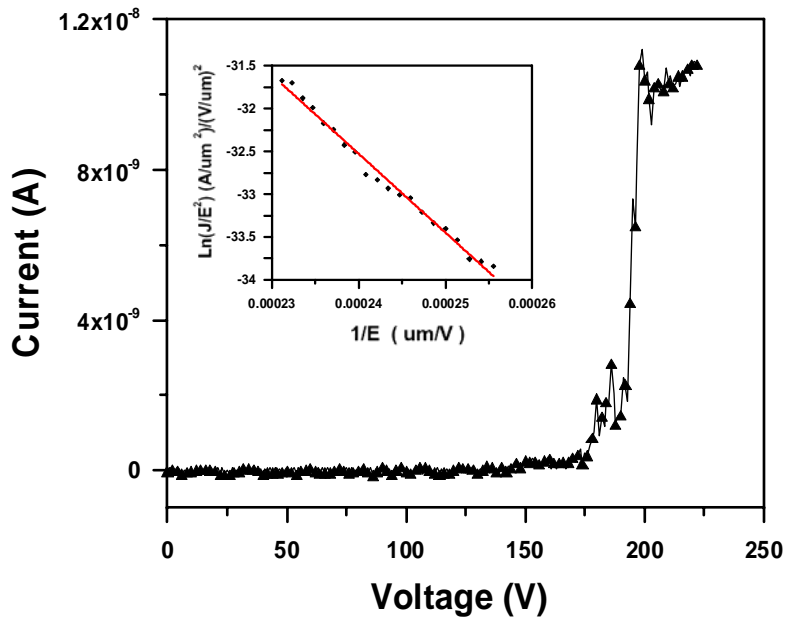


(b)

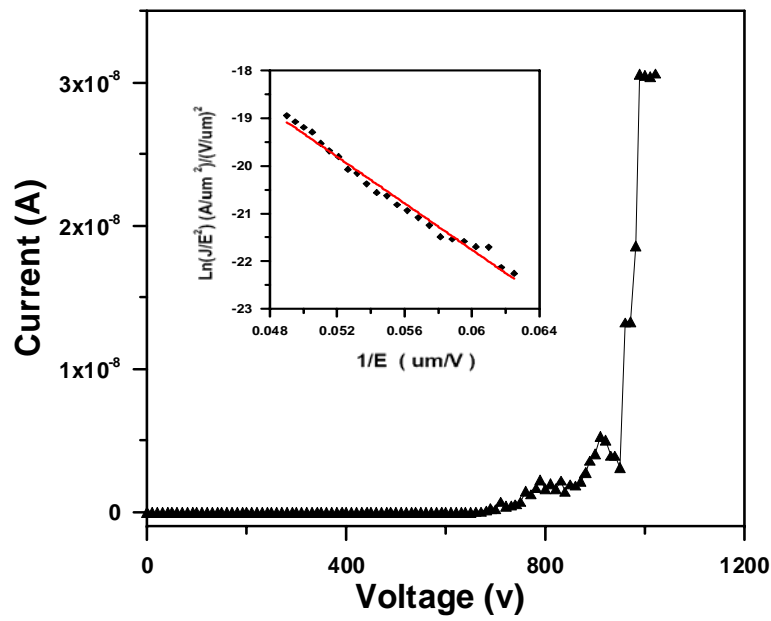


(c)

Fig. 1 SEM images of (a) Si nanotips array after dry plasma etching with height of $20\mu\text{m}$ and (b) the image of tungsten anode in SEM instrument. (c) Field emission is measured by aligning the emitter apex and the anode apex for a small separation by SEM. The top tip is the tungstenic anode and the below tip is the Si emitter.

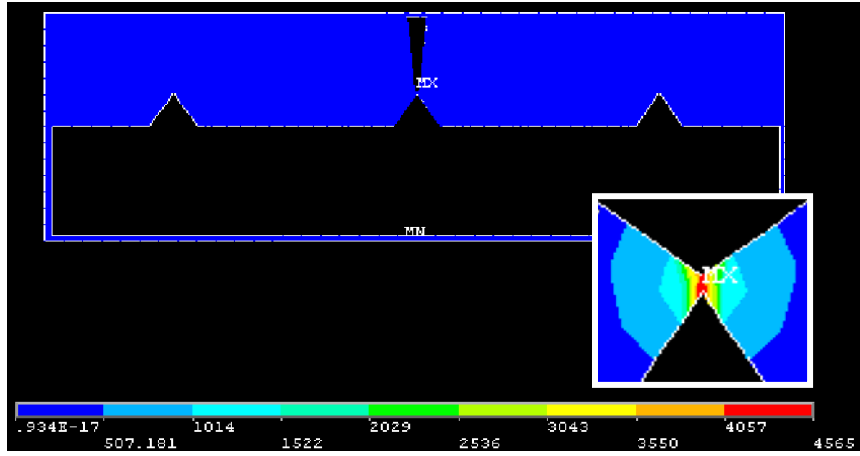


(a)

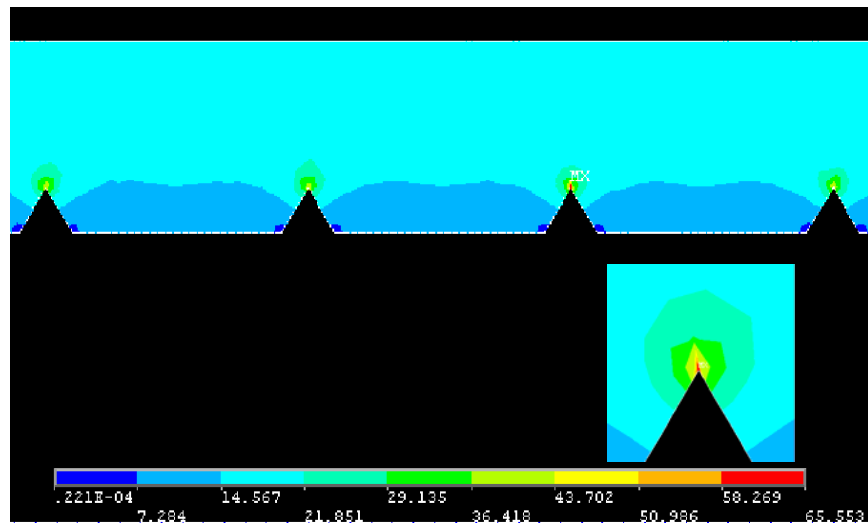


(b)

Fig. 2 Field emission behavior of (a) a single emitter for distance 46nm between the emitter and the sharp anode. Analysis using Fowler-Nordheim model shown in the inset indicates the emitter can be turned on at [that the turned-on field is estimated as $E_0 = 4065 \text{ V/um}$. (3913.043) (b) the result of average measurement with distance 50um between the emitters and the flat anode. The turned-on field analyzing from the inset graph is estimated as 11.7 V/um .



(a)



(b)

Fig. 3 Simulated results of the electrostatic field between the silicon emitter and (a) tungsten nano anode, (b) large flat anode.